

Van Meirvenne, De Corte, Boel, and Taerwe

2017 PCI/NBC

NONLINEAR ANALYSIS OF THE END ZONES OF PRESTRESSED CONCRETE GIRDERS

Kizzy Van Meirvenne, Department of structural engineering, Ghent University, Belgium

Wouter De Corte, PhD, Department of structural engineering, Ghent University,
Belgium

Veerle Boel, PhD, Department of structural engineering, Ghent University, Belgium

Luc Taerwe, PhD, Department of structural engineering, Ghent University, Belgium

ABSTRACT

Pretensioned concrete girders have been used for many years in construction. Nevertheless, optimization is still possible, especially regarding the anchorage zones. These are typically subjected to different types of stresses due to the local transmission of the prestressing force. By using a 3D nonlinear finite element model, the stresses and cracks in the anchorage zone due to the prestressing forces can be predicted in a more reliable manner. In this paper two 3D FE models are developed by using the concrete damage plasticity model in Abaqus. In the first model, the load transfer is defined by creating a shear force around each strand. In the second model, the interaction between the strands and the concrete is created by using surface-to-surface contact elements with friction. Finally, to validate the models, the results are compared with strain measurements on a precast beam during production at a precast concrete plant.

Keywords:

Pretensioned Girders, End Zones, FEM, Abaqus

INTRODUCTION

Pretensioned concrete girders have been used for many years in construction. Nevertheless, there is a lack of unified and practical guidelines for the calculation of the reinforcement in the anchorage zones. The current guidelines as the Eurocode [1], fib Model Code [2], ACI [3] and AASHTOO [4], make use of simplified linear analytical calculation methods or strut-and-tie models. However, only nonlinear models predict the stresses and crack formation in a more reliable manner. Okumus [5] demonstrates this by comparing linear and nonlinear FE calculations of a precast prestressed bridge girder. The two models behave in a similar way until the concrete elements reach their theoretical tensile strength. Once cracking in the concrete occurs, a redistribution of stresses takes place and the rebars become engaged. The linear models largely underestimate the strains in the concrete, since these models do not consider the stiffness loss of concrete upon cracking.

In this paper nonlinear FEA is used to estimate the probability of crack formation and the stress distribution at the girder ends after prestress release. Two different ways of modeling the prestress transfer, based on respectively Okumus et al. [5] and Abdelatif et al. [6] are implemented and compared with DEMEC measurements on a full-size girder in a precast concrete plant.

LITARATURE OVERVIEW

Although end zones of precast pretensioned girders have been examined for many years, only recently a growing number of researchers attempts to study this with nonlinear finite element models. Okumus et al. [5] investigate the end zones of prestressed concrete bridge girders by the use of a nonlinear concrete model. They modeled I-shaped girders using the concrete damaged plasticity model in the region with a distance equal to the girder depth from the end of the girder. The prestress force was applied by modeling the strands as gaps in the concrete and applying a tangential surface stress along the strand surface over the transfer length. The applied shear stress was distributed in two different ways, linear and uniform, and the first distribution is concluded to be acceptable. Although the Hoyer effect is not taken in account, the model can be seen as an acceptable simplification. In contrast to Okumus [5], Arab et al.[7] attempted to model the strand as a physical element. They also work with the concrete damaged plasticity model in Abaqus, but the strands are modeled by two different methods, the embedded technique and the extrusion technique. In the first technique, the strands are modeled by 1D-truss elements and are assumed to be embedded into the concrete, which is modeled by solid elements. Although this model seems to contain a feasible methodology and has less computational cost, the methodology renders fewer details regarding the interface between the strands and the concrete, such as the slip and the transfer length. In the extrusion technique the interactions between the strand and the concrete are defined using surface-to-surface elements. Furthermore, normal and tangential behavior properties between the concrete and the strand as the coefficient of friction μ and 'hard' contact are defined. The 'hard' contact is mathematically enhanced by the lagrange multiplier technique. The modeling approaches are verified based on selected experimental data of Akhnoukh [8]. This way of modeling the end zone of prestressed girders seems to be an appropriate method, not only based on the results of Arab's work, but also on the work of Abdelatif et al. [6]. Abdelatif et al. [6] also make use of the concrete damage plasticity model, although they use the software package Ansys instead of Abaqus. In that work,

they did not only present a 3D nonlinear finite element model with interaction between strand and concrete but they also proposed an analytical model based on the thick-walled cylinder theory. Moreover the impact of the diameter of the prestressing steel, the concrete cover, the concrete strength, the initial prestress and many other parameters are examined in a parametric study. It is noteworthy to mention that both authors propose different values for the coefficient of friction. Abdelatif et al. [6] uses a value of 0.4, whereas Arab et al. [7] prescribes a coefficient of friction between 0.7 and 1.4. In 2015, Yapar et al. [9] propose the most recent attempt to develop a 3D finite element model for a prestressed concrete girder. A comparison between results obtained by numerical modeling and by an experimental 4-point bending test was performed. Deformations as well as crack formations were compared and lead to corresponding results. However, it is remarkable that the strands are modeled using equivalent rectangular cross sections. The aim of the model was not in particular to investigate the transfer of the stresses from the pretensioned strand to the concrete, but to investigate the global behavior after the prestressed girder has been loaded. For this reason, the modeling method of the strands by Arab et al.[7] (extrusion technique) and Abdelatif et al. [6] seem to be the most useful method to model and analyze the end zone. Both models are however applied with only one strand in a concrete rectangular section. The study of this paper is based on the same modeling principles but is applied on a full-size girder with multiple strands and compared with the results of the same girder produced at a precast concrete plant. As mentioned before, not only the strand modeling method suggested by Abdelatif et al. [6] will be used but also the simplified method of Okumus et al. [5].

EXPERIMENTAL TEST

In order to validate the finite element models, an experimental test is carried out at a concrete precast plant during regular production. The test girder consists of an I-shaped cross-section with a height of 600 mm, a width of 325 mm and 10 strands in cross section. Both girder ends were equipped with an end block with a length of 600 mm. In addition, a transition zone of 200 mm is provided between the I-shaped cross section and the end block. A sketch of the geometry is presented in figure 1.

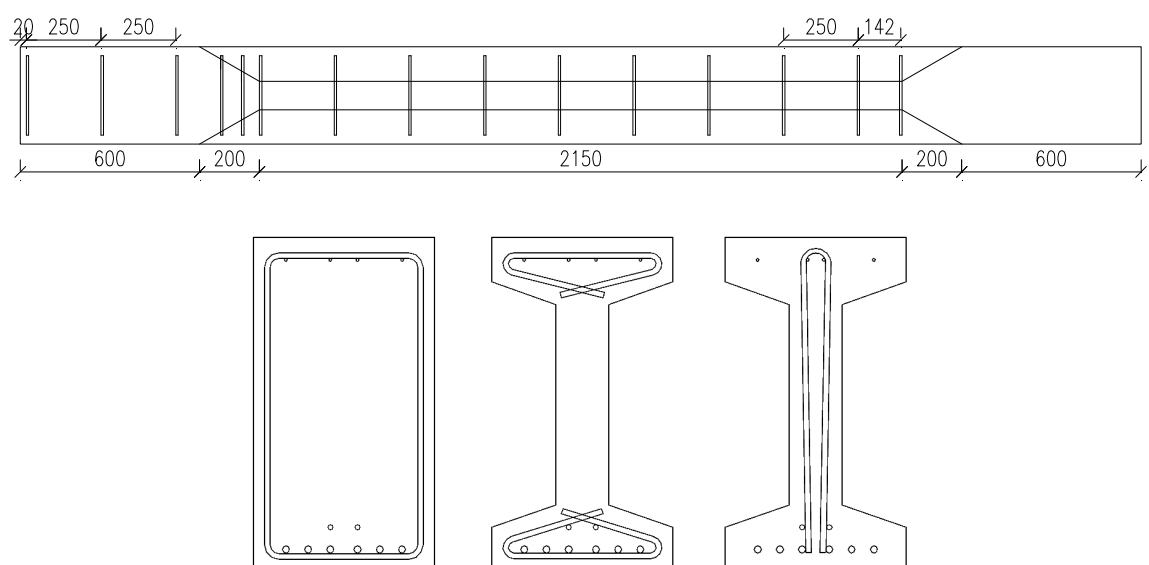


Fig. 1 Geometry of the test girder [mm]

The end zones of the girder are both reinforced in a different way. The right hand side on figure 1, also the active side of the beam, is produced without reinforcement. The other side, on the contrary, is produced with a minimal reinforcement consisting of three rectangular stirrups with a diameter of 8 mm every 250 mm, followed by two smaller rectangular stirrups with the same diameter. Subsequently, in the I-shaped cross section, I-shaped stirrups with a diameter of 8 mm were installed every 250 mm. In this way, two different tests could be carried out on the same beam. Moreover, in the cross section of the girder three different types of strands are present, each with a different pretension force as summarized in table 1. The strands were produced with an invariable eccentricity to the center of gravity of the beam.

Table. 1 characteristics of the strands

Strand	Diameter [mm]	A_p [mm ²]	f_{pk} [N/mm ²]	Prestress force [kN]
5 mm	5,2	13,6	1960	21,3
3/8"	9,3	52	1860	77,4
1/2"	12,5	93	1860	138,4

The girder is cast with self-compacting concrete of grade C55/67. After three days the prestress strands are released. At the plant, three compressing tests were carried out at three days and three tests at 21 days, which is a small deviation of the standard procedure at 28 days. Therefore, the results of the cubes at 21 days of 150x150x150 mm, preserved under water by a temperature of 20°C, were recalculated to 28 days using the Fib Model Code [2]. The compressive strength of the cubes at 21 days was 69.2, 68.0 and 62.1 N/mm² respectively, resulting in an average of 66.4 N/mm². This average is used to calculate the concrete compressive (f_{cm}) and tensile strength (f_{ctm}) at 28 days and subsequently at three days. With a value of 0.20 for the s-factor, the concrete tensile strength and the compressive strength after three days are calculated as $f_{ctm} = 2.56$ N/mm² and $f_{cm} = 51.8$ N/mm². The latter results are used as input parameters for the concrete damaged plasticity model. Instead of the recalculated values of 21 days to three days, the experimental value of three days may also be used. However, this will not be discussed in this paper.

$$f_{cm} = 0.79 \cdot f_{ccubm} \quad (1)$$

$$f_{cm}(t) = \beta_{cc}(t) \cdot f_{cm} \quad (2)$$

$$\beta_{cc}(t) = \exp \left\{ s \cdot \left[1 - \left(\frac{28}{t} \right)^{0.5} \right] \right\} \quad (3)$$

$$f_{ck} = f_{cm} - 8 \quad (4)$$

$$f_{ctm} = 0.30 \cdot f_{ck}^{2/3} \quad (5)$$

$$f_{ctm}(t) = \beta_{cc}(t) \cdot f_{ctm} \quad (6)$$

t	age of the concrete [days]
s	coefficient which depends on the strength class of the cement and the hardening characteristics [-]
$f_{ctm}(t)$	concrete tensile strength at t days [MPa]
f_{ctm}	concrete tensile strength at 28 days [MPa]
f_{ck}	characteristic value of f_c [MPa]
f_{ccubm}	Average cubic compressive concrete strength [MPa]

In order to measure the strains in the end zones, several measuring points were attached to the concrete cover with a non-shrink adhesive, as presented in figure 2. With an invar reference bar, provided with two conical locating points, the measurement points were placed at a fixed distance of 100 mm. Near the end face of the beam the measuring points were placed in overlay, with an intermediate distance of 50 mm in order to obtain more accurate results near the beam end. In the vertical direction, the reference points starts at a distance of 50 mm of the underside of the girder and in the horizontal direction at 25 mm of the end face of the girder. The exact distance between the reference points was then measured with a DEMEC mechanical strain gauge with a basis of 100 mm and a 16 microstrain resolution. The distance is measured before and after the prestress release. In this way the strains can be calculated at different locations.



Fig. 2 Measurement locations

The results of the horizontal measurements of the reinforced end zone are visualized in figure 3. From these, only the results at a height of 50 and 100 mm of the bottom of the girder will be compared with the 3D finite element models.

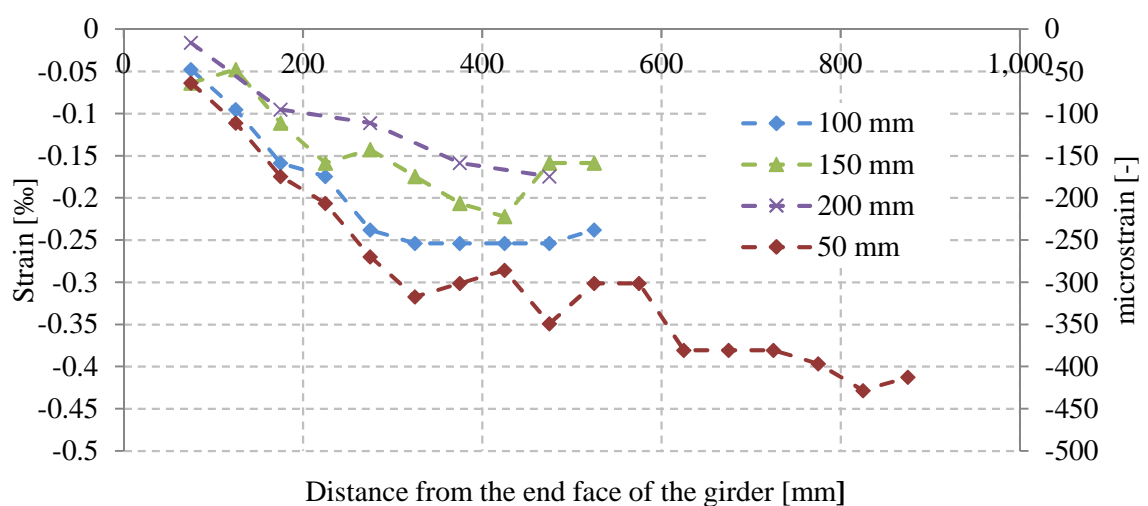


Fig. 3 Measured strain at the end zone

FINITE ELEMENT MODELS

MATERIAL MODELS

Concrete

The concrete material parameters are based on the concrete damaged plasticity model as used in Abaqus [10]. This model is appropriate for simulating the nonlinear behavior of concrete in compression as well as in tension. The CDP model is based on the Drucker-Prager hypothesis. An overview of the used input parameters of the concrete model are given in Table 2.

Table. 2 Material properties of concrete

Density ρ [kg/m ³]	2500
Poisson ν_s [-]	0.2
Dilatation angle [°]	30
Excentricity [mm]	0.1
f_{b0}/f_{c0} [-]	1.16
K [-]	0.666

Beside the general material properties, the CDP model requires several specific input parameters. These define the compressive and the tensile behavior, respectively. The compressive behavior was modeled as a combination of experimental results and theoretical formulas. Figure 4 demonstrates the used CDP with on the left hand side the compression input parameters and the two figures on the right hand side represent the tensile behavior.

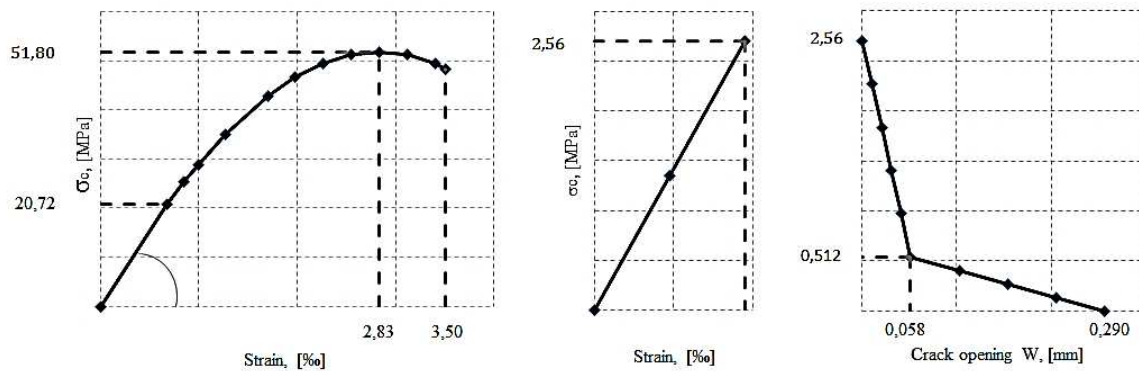


Fig. 4 Used concrete damaged plasticity model

Steel

The steel was modeled as a linear material. Because the stress in the pretensioning steel is always lower than the yield stress, the linear material properties are justified. The calculation model requires the input of several material properties as the volumetric density, the modulus of elasticity and the Poisson ratio. These characteristics are listed in table 3. Both for the stirrup reinforcement as for the prestressed strands the same properties were used.

Table. 3 Material properties of steel

Density ρ [kg/m ³]	7800
Modulus of elasticity E_s [MPa]	200000
Poisson ratio ν_s [-]	0.3

GENERAL MODEL

The modeled girder consists of 3 different parts: the end block (1), the I-shaped girder (2) and the transition element (3) which are all tied together (see figure 5). In each part circular cut-outs were provided at the positions of the strands. Due to symmetry, only one fourth of the beam needed modeling (see figure 6). This reduces the computing time and the calculation memory in a significant manner.

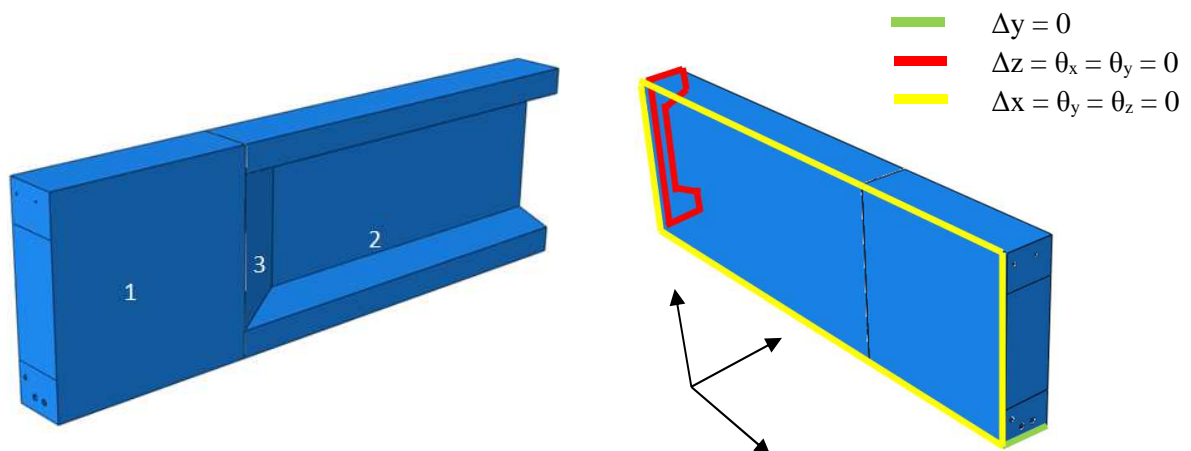


Fig. 5 Geometry of the modeled girder

Fig. 6 Boundary conditions

In order to be able to calculate the stresses, the girder is meshed into smaller 3D elements. Since the largest stress gradients occur at the end of the beam, the girder is meshed densely at the girder end and the mesh size is gradually increased away from the girder end, which is shown in figure 7. For the concrete beam hexagonal elements (C3D8R, 8-node linear brick elements with reduced integration) are used whereas for the strands, wedge type elements (C3D6, 6-node linear triangular prism elements) are selected. The quadratic type element requires a larger computational cost and results only in a negligible improvement in accuracy.

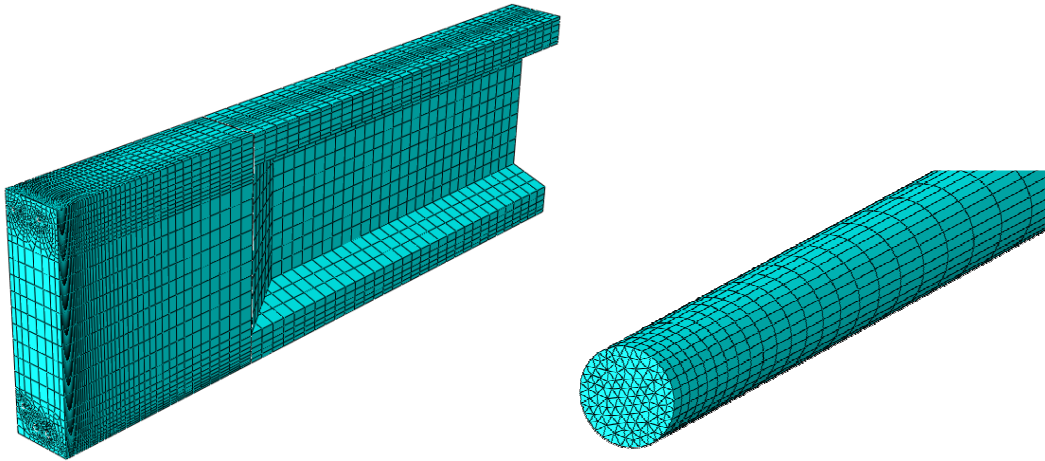


Fig. 7 Mesh of the girder and the strand

LOAD TRANSFER

As mentioned in the literature overview, two different ways of load transfer are modeled. Both methods will be clarified in the next part.

➤ Classic shear based model

In this way of modeling the load transfer is defined as a shear stress along the strand surface over the transfer length. In this model, the strands are tied to the surrounding concrete. The transfer length is a widely discussed topic in literature [12]. Many researchers examined this length and different formulas are developed which results in a wide scatter on the values [13]. In this paper it is opted to consider the transfer length which is calculated applying the formula of the Fib Model Code [11,12]. The transfer length calculated in this way as well as a 50% larger transfer length are modeled. The reason for doing so, is the large range of transfer length as explained before. The transfer length according to the Fib Model Code [11] is calculated with equation 7.

$$l_{bpt} = \alpha_{p1} \cdot \alpha_{p2} \cdot \alpha_{p3} \cdot \frac{A_p}{\pi \cdot \phi} \cdot \frac{\sigma_{pi}}{\eta_{p1} \cdot \eta_{p2} \cdot f_{ctdi}} \quad (7)$$

In this α_{p1} is a value which takes into account the method of the force transfer, and a gradual force transfer results in a value of 1. For the parameter α_{p2} a value of 0.5 is proposed in the case strands are used. Moreover, A_p is the cross-sectional area of the tendon, ϕ is the nominal diameter of the tendon and σ_{pi} is the steel stress just after release which is considered as $0.7 f_{pk}$, with f_{pk} is the characteristic value of tension yield stress of prestressing steel assumed as 1860 N/mm^2 for $1/2''$, 1960 N/mm^2 for $3/8''$, and 5 mm strands. Parameter η_{p2} takes the type of the prestressing tendons into account. The Fib Model Code 2010 [11] proposes the value of 1.2 for a 7-wire strand. The position of the tendons is taken into account by η_{p1} , where for horizontal tendons a value of 1 is prescribed. The transmission lengths are given in **Fout! Verwijzingsbron niet gevonden.4.**

Table. 4 Transfer Length according to Model code 2010 [11]

	1/2 " (12.5 mm)	3/8 " (9.3 mm)	5 mm (5.2 mm)
Transfer length [mm]	502.0	377.0	175.8
Transfer length [mm] + 50%	753.0	565.5	263.6

In order to model the shear stress along the strand, an analytical field is defined in Abaqus. The shear stress is calculated by dividing the prestress force by the perimeter of the strand and the transfer length. Three different models are developed for each strand. Firstly, a function linearly decreasing towards zero over the transfer length is modeled. Secondly, a similar linearly decreasing function reaching zero at a length which is 50% larger is used. The third modeled function is a bilinear function with a maximum at 20% of the transfer length. The first and last mentioned function are visualized in figure 8. As Okumus et al. [5] concluded that uniform stress distribution is less accurate to model the shear stress, this model is not considered in this paper.

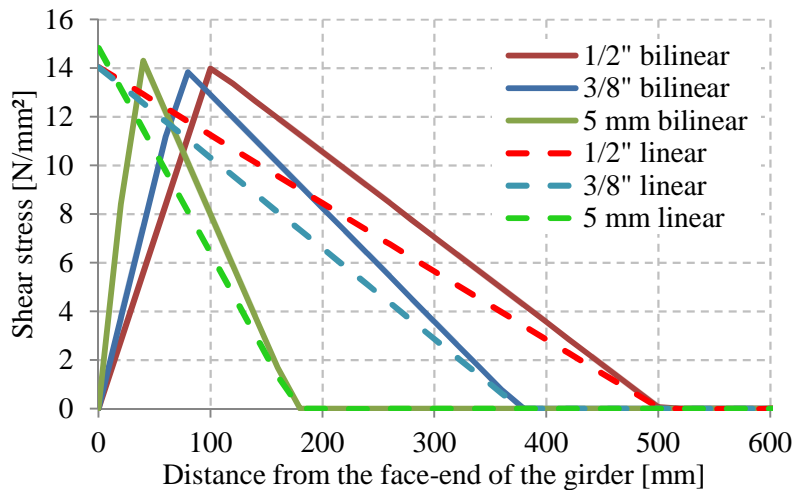


Fig. 8 Analytical fields

➤ Model with friction

In the second configuration the pretensioning stress is modeled as a predefined field. Since there were three different strands each with another prestressing force, three separate fields are specified. The interaction between the concrete and the prestressing strands is defined in tangential and normal direction. In the direction along the strand (tangent) the Coulomb friction law was used to define the frictional behavior, and the most important parameter to be specified is the coefficient of friction. The latter parameter is an unknown variable, so different values were taken into consideration. In the normal direction a hard contact needs to be chosen. This default pressure-over closure relationship used by Abaqus implies that the surfaces transmit no contact pressure unless the nodes of the slave surface contact the master surface. There is no penetration allowed at each constraint location as well as no limit to the magnitude of contact pressure that

can be transmitted when the surfaces are in contact [10]. Furthermore, the Augmented Lagrange algorithm was set active. In a last stage, the interaction is defined as a surface-to-surface contact.

Because of the large number of material parameters a lot of scatter of the results is possible. An extensive parametric study, as Abdelatif et al. [6] did for a model with one strand, is highly recommended. In this paper, one of the most important parameters, the coefficient of friction, is studied.

COMPARISON OF EXPERIMENTAL AND FEM RESULTS

Firstly the results of the experimental test at a height of 50 mm (figure 9) and 100 mm (figure 10) from the bottom of the beam are compared with the results of the shear transfer based and friction based models. As mentioned, the latter model is calculated with different coefficients of friction. From the first graph it can be determined that the linear and bilinear results are creating an upper limit of strains. Furthermore, the results of the linear model with a 50% larger transfer length and the friction based models with a friction coefficient between 0.8 and 1.2 have a curve shape similar to the experimental curve, whereas, the models with a lower value for the friction coefficient have a rather different shape.

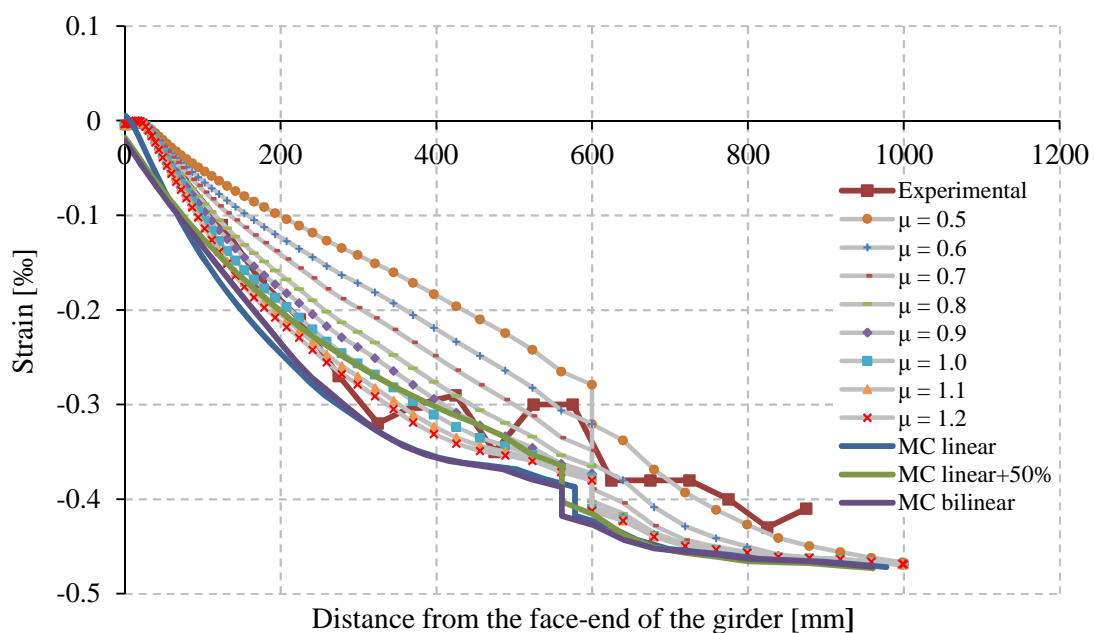


Fig. 9 Experimental and analytical results of the strains at 50 mm from the bottom of the girder

In figure 10, an identical trend can be observed. In this figure the linear model is once more represented by the upper limit of strains. Furthermore, the models with a coefficient between 0.8 and 1.2 have a similar shape as the model with a 50% larger transfer length. It must be noticed that in this situation the experimental values have a lower position compared to the analytical values.

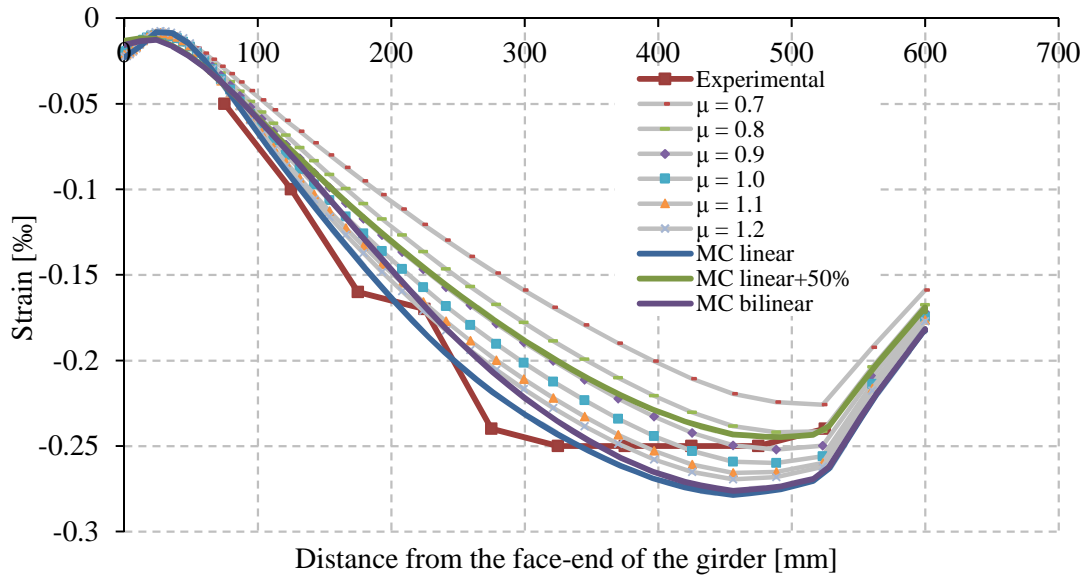


Fig. 10 Experimental and analytical results of the strains at 100 mm from the bottom of the girder

It can be questioned whether a similar slope would result in the same transversal stresses which lead to cracks in the end face of the girder. In order to solve this question two steps were taken into consideration. In the first step, the transfer lengths of the friction based models were investigated. In the second step, the vertical stresses were measured in the finite element models.

The transfer length is measured by investigating the longitudinal stresses on the edge of the strand. This length can be estimated at the intersection of a horizontal line at 95% of the maximum stress. According to the results from a 1/2" strand, visualized in figure 11, it can be concluded that a higher coefficient of friction results in a lower transfer length. Figure 11 illustrates also the fact that there is no linear distribution between the transfer length and the coefficient of friction.

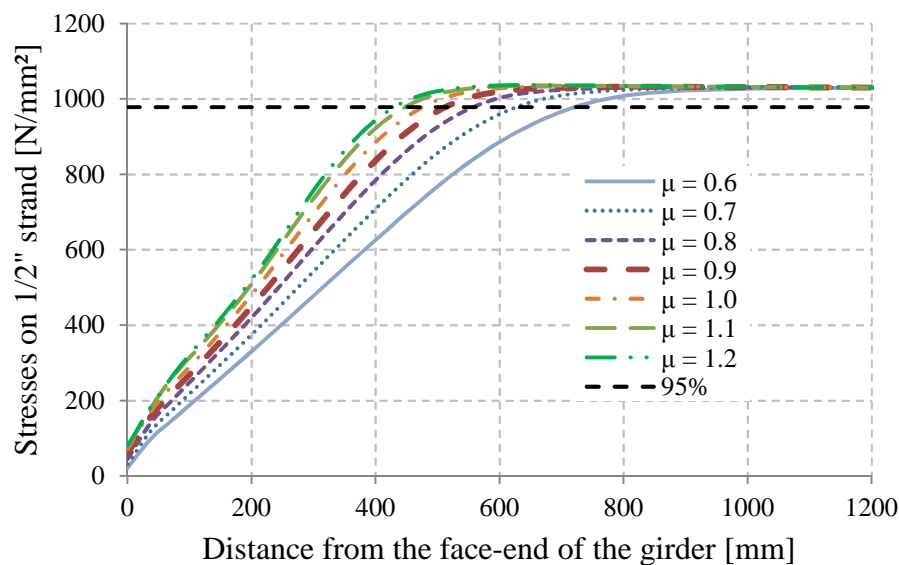


Fig. 11 Transfer length with a varying coefficient of friction

In a next step, the vertical stresses are measured in each model at a certain height over approximately 150 mm from the end of the girder. In this way the occurring vertical splitting force, which leads to cracks in the end zones, can be calculated. Figure 12 depicts that vertical stresses at the concrete surface are calculated at a height of 250 mm and 300 mm counted from the bottom of the beam. The tensile stress distribution along the mentioned height of 250 mm is displayed in figure 13.

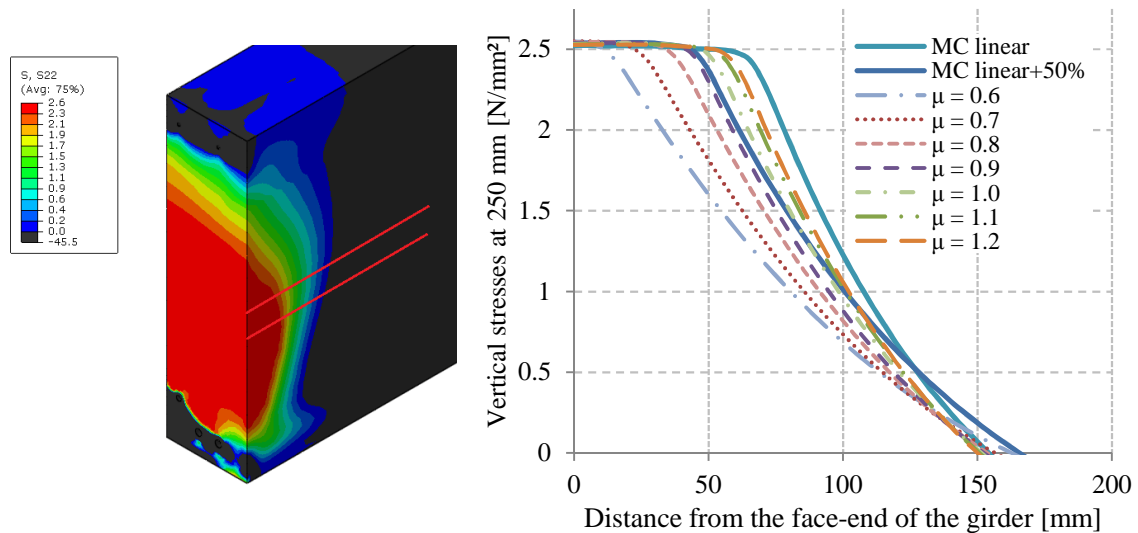


Fig. 12 Location of the calculated vertical stresses **Fig. 13** Vertical stresses at 250 mm [N/mm²]

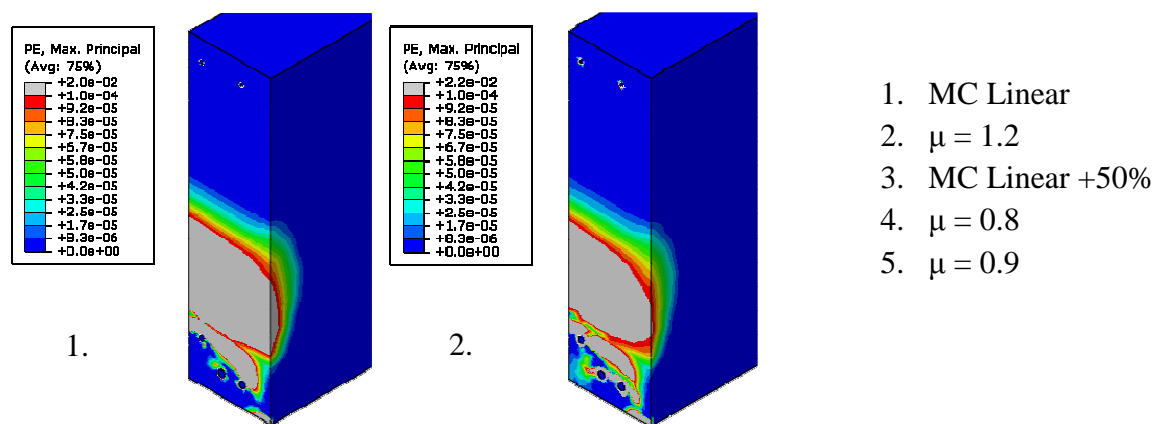
Subsequently, the vertical splitting force can be calculated by making the sum of, the integral of the vertical stress multiplied with the width of the beam, and the forces in the modeled reinforcement. At the earlier mentioned heights of 250 and 300mm, the forces are calculated for the different models and they are summarized in table 5. For the shear based models two values for the transfer length are given in the table, the first one is the modeled length and the second one is 95% of this length. When analyzing the values in the table, it can be seen that it is indeed correct to assume that the linear shear based model results in the largest vertical splitting force. This linear shear based model emerges also as the upper bound in figure 9 and 10. In these figures, the shear based model with the larger transfer length is most similar to the friction based models with a coefficient between 0.8 and 1. Depending on the level where the vertical stresses are determined, different values can be found.

Table. 5 Calculated splitting force

	95% L _{bpt} [mm]		Vertical Force 250 mm [kN]	Force in the rebars [kN]	Total Force 250 mm[kN]	Vertical Force 300 mm [kN]	Total Force 300 mm[kN]
	502	476.9					
MC linear	502	476.9	83.5	3.4	86.9	84.6	88.0
MC bilinear	502	476.9	84.9	3.3	88.2	84.5	87.8
MC lin.+50%	753	715.4	77.3	2.4	79.7	76.4	78.8
μ = 0.6	722.6		59.5	2.1	61.7	60.2	62.3
μ = 0.7	627.6		64.2	2.4	66.7	65.5	67.9
μ = 0.8	557.5		69.4	2.7	72.1	71.2	73.9
μ = 0.9	513.5		72.6	2.8	75.4	74.6	77.4
μ = 1.0	476.8		75.7	3.0	78.7	77.9	80.9
μ = 1.1	447.4		78.0	3.1	81.2	80.3	83.5
μ = 1.2	431.9		79.0	3.2	82.2	81.5	84.8

This is the reason why the vertical forces for these particular models were calculated at different levels spacing 5 mm, starting from the bottom of the beam. The results of this calculation show that the maximum value of the shear based model is 80.5 kN measured at a height of 275 mm. For the friction based models the maximum values are 73.9 kN, 77.5 kN and 81.1 kN for the friction coefficients 0.8, 0.9 and 1 respectively. This implies that the spalling force of the shear based model is 0.7% smaller and 3.7% larger than the friction based models with the coefficient of 0.9 and 1 respectively. These results suggest that both models predict the spalling force in a similar way. However, it is noteworthy that the transfer lengths do not correspond in a similar way. This is probably due to the fact that the transfer length is defined differently. In the first model, the transfer length is the length where the shear stress is zero. In the second model, on the contrary, the transfer length is 95% of the maximal stress in the strand. This stress is lower than the initially applied stress. For example, on the 1/2" strand a predefined stress of 1128 N/mm² was applied while the maximum measured stress in the strand is 1029 N/mm². This means that it is highly probable that the model takes prestress losses into account.

As a last part of the comparison between the experimental and analytical data, the plastic strain, which is an indication of the damaged zone, is investigated. In the earlier mentioned results, the linear model shows the highest spalling force followed by the model with a friction coefficient of 1.2. The same result can be considered regarding figure 14, because a larger spalling force results in a larger damaged zone. To be complete, the linear model with the larger transfer length is also taken into consideration. The magnitude where the plastic strain has a value higher than 1e-4, is situated between the models with coefficients of 0.8 and 0.9. However during, and shortly after, the experimental test, no cracks occurred. In order to make a conclusion for the most feasible transfer length or friction coefficient, the DEMEC measurements are not accurate enough.



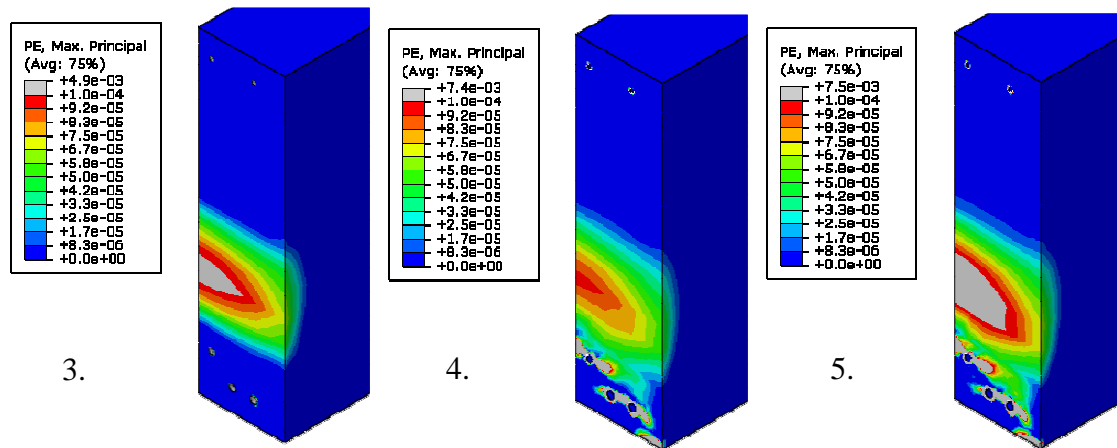


Fig. 14 Results of the plastic strain

CONCLUSION

This paper starts with experimental tests on a full size girder in a precast concrete plant. The tests consist of DEMEC measurements on the side of the girder. This is followed by modeling the load transfer in two different ways, namely shear and friction based. The first model is based on the work of Okumus et al.[5] where no rectangular end zone was considered. Okumus et al.[5] modeled an I-shaped end zone whereas in this work a rectangular zone is modeled. For the second model the principles are based on the work of Abdelatif et al. [6]. In this paper the model is extended with multiple strands. Out of the comparison between the experimental and analytical models, two conclusions can be taken. Firstly, the results of the linear model with a 50% larger transfer length as calculated by the Fib Model Code and the friction based models with a friction coefficient between 0.8 and 1.2 have a similar curved shape. This is also reflected in the results for the calculated spalling force and the areas where the plastic strain has a value higher than $1e-4$. A second conclusion can be made looking at the results of the linear shear based model and the model with a coefficient of friction of 1.2. The first mentioned model is the upper limit in the results. This is also reflected in the results because it has the highest values for the spalling force and the plastic strain area. These values are similar to the results of the model with the friction coefficient of 1.2, which is the nearest graph to the linear shear based model. The fact that the transfer lengths of the mentioned models do not correspond which each other can presumably be explained by the applied definition of this parameter. In the shear based model, the transfer length is the length where the shear stress is zero. In the friction based model, on the contrary, the transfer length is 95% of the maximum stress in the strand. This stress is lower than the initially applied stress, which means it is highly probable that the model takes losses into account. As a main conclusion, it can be said that these results suggest that the two different ways of modeling gives a similar result, although, the shear based model is a simplified model and does not take the Hoyer effect into account. Unfortunately, both models have an unknown factor. The transfer length in the first model and the coefficient of friction in the second model. The value for this latter parameter is in this work assumed to be in a range of 0.8 to 1.2. However, defining the value for this parameter out of one experiment would be too premature. A next and comprehensive experimental test will bring definite answers.

ACKNOWLEDGMENTS

This research was supported by the Agency for Innovation by Science and Technology (IWT) and the company Structo+, producers of reinforced and prestressed beams, columns, floor elements, roof elements and bridge girders. The authors wish to express their gratitude for the support.

REFERENCES

1. CEN. Eurocode 2: design of concrete structures – Part 1–1: general rules and rules for buildings. European standard EN 1992-1-1:2004: Brussels: Comité Européen de Normalisation, 2004.
2. Comité-Euro-International du Béton, Model Code 2010, Lausanne: Fib, 2011.
3. ACI Committee 318. Building code requirements for reinforced concrete (ACI 318-11). Farmington Hills, MI: American Concrete Institute, 2011.
4. American Association of State Highway and Transportation Officials, AASHTO LRFD 2012 Bridge Design Specifications, (6), pp. 5-168 - 5-169, 2012.
5. Okumus P, Oliva and Becker, “Nonlinear finite element modeling of cracking at ends of pretensioned bridge girders.” *Engineering Structures* 40, pp. 267-275, 2012.
6. Abdelatif J, Owen and Hussein, “Modelling the prestress transfer in pre-tensioned concrete elements,” *Finite Elements in Analysis and Design*, pp. 47-63, 2015.
7. Arab A, Badie and Manzari, “A methodological approach for finite element modeling of pretensioned concrete members at the release of pretensioning,” *Engineering Structures*, 33 (1918-1929), 2011.
8. Akhnoukh AK, “Development of high performance precast/prestressed bridge girders. Doctoral dissertation.” Department of Civil Engineering. University of Nebraska-Lincoln, 2008.
9. Yapar O, Basu and Nordendale, “Accurate finite element modeling of pretensioned prestressed concrete beams,” *Engineering Structures*, pp. 163-178, 2015.
10. Dassault Systèmes Simulia Corporations, Abaqus analysis user's manual, Providence: Simulia, 2012.
11. FIB. Model Code 2010. First complete draft. Fib Bulletin No. 55, vol. 1. Lausanne: International Federation for Structural Concrete, 2010.
12. Martí-Vargas J.R., Serna, Navarro-Gregori, Pallarés, “Bond of 13 mm prestressing steel strands in pretensioned concrete members.” *Engineering Structures* 41, pp.403–412, 2012.
13. Van Meirvenne K, De Corte, Boel, Taerwe, “Numerical and experimental analysis of the transfer length and its influence on the anchorage zone design of pretensioned concrete.” CTU congress, Dundee 2016 (to be published).